SEMARAK ILMU PUBLISHING

Semarak International Journal of Electronic System Engineering

Journal homepage:
https://semarakilmu.my/index.php/sijese/index
ISSN: 3030-5519

Oil Palm Detection and Health Classification from UAV Multispectral Images using You Only Look Once (YOLO)

Abraham Lim Bing Sern[1], Nor Azuana Ramli[1,*], Wan Mohd Rozaimi Wan Mustafa[2], Suraj Arya[3]

[1] Centre for Mathematical Sciences, Universiti Malaysia Pahang Al-Sultan Abdullah, Kuantan, Pahang, Malaysia
[2] MySpatial Sdn Bhd, MTDC Technology Centre, Universiti Putra Malaysia, Co9P Drone and Geospatial Technology Centre Level 1, Co9P Idea Tower, 1, UPM, 43400 Seri Kembangan, Selangor, Malaysia
[3] Department of Computer Science and Information Technology, Central University of Haryana, India

ARTICLE INFO

Article history:
Received 14 April 2025
Received in revised form 10 May 2025
Accepted 21 May 2025
Available online 30 June 2025

Keywords:
Oil palm; object detection; image recognition

ABSTRACT

Elaeis guineensis is a tropical plant that originated in West Africa but is currently widely grown in many tropical places worldwide, including Malaysia. Malaysia is the world's second-largest palm oil exporter; hence, the government is willing to allocate RM100 million to the 2024 budget. With that budget allocation, palm oil production is expected to increase this year. However, the industry faces several problems and challenges involving palm oil, such as diseases caused by pests, the damage caused by rats, and the effects of climate change. It is necessary to overcome these problems and challenges to ensure the sustainability of palm oil production. One of the solutions is to apply remote sensing technology to monitor the health of oil palm trees. This study was conducted with the main objective of developing a model that is able to detect oil palm trees and classify their health by using You Only Look Once (YOLO). The dataset used for this study was collected from a site visit in Terengganu. Then, the dataset underwent pre-processing, such as auto-oriented, resizing, bounding boxes, and labelling. There are two categories for the health classification: healthy and unhealthy. The study was carried out by training a custom model with both YOLOv8 and YOLOv9 independently to consider which model performs better in precision, recall, mAP50, and mAP50-95. The results of YOLOv8 were a precision score of 58.7%, a recall value of 84.9%, a mAP50 of 71.3%, and a mAP50-95 of 48.9%, while YOLOv9 had a precision score of 64.1%, a recall value of 80.4%, a mAP50 of 72.6%, and a mAP50-95 of 50.2%. It was observed from the experiment conducted that YOLOv9 gave a better result than YOLOv8 in terms of precision, mAP50, and mAP50-95 overall, while YOLOv8 had a higher recall value during testing than YOLOv9. In addition, this study recommended implementing semi-automated systems, which combine automated processes with human oversight and apply augmentation techniques to enhance model resilience against variability.

* *Corresponding author.*
E-mail address: azuana@umpsa.edu.my

https://doi.org/10.37934/sijese.6.1.1937

1. Introduction

Elaeis guineensis, or oil palm, originated in West Africa and is now widely cultivated in tropical regions due to its high oil yield. Indonesia and Malaysia produce about 83% of the global palm oil. While unsustainable practices offer economic benefits, they also raise significant health and environmental concerns. Currently, artificial intelligence (AI) and drone technology are being utilised in agriculture to enhance efficiency, decrease reliance on labour, and improve palm oil quality and monitoring [1].

Agricultural production increased four times between 1960 and 2015 due to Green Revolution technology and expanded resource use [2]. Malaysia is the second-largest palm oil producer, although it has faced challenges such as pests, diseases like Basal Stem Rot (BSR), climate change, and economic disruptions [3]. Climate change threatens palm oil cultivation by reducing biodiversity and limiting plantation areas [4]. Events like the Coronavirus disease 2019 (COVID-19) and political issues have also impacted palm oil prices and exports. Rats, including wood, black, and rice rats, also contribute to crop damage [5]. Sustainable practices and technological innovations are crucial for the long-term success of Malaysia's palm oil industry [6].

Oil palm diseases affect various plant parts and are caused by pathogens, pests, and nutrient imbalances, leading to reduced yield and quality [7,8]. Traditional monitoring methods are time-consuming and limited in coverage, while drones offer a smart farming solution but face challenges like high costs, sensor limitations, and complex data analysis [9]. In recent years, the convolutional neural network (CNN)-based deep learning technique has significantly enhanced object detection performance [10]. A faster Region-based Convolutional Neural Network (R-CNN), introduced in 2015, improves object detection by integrating a Region Proposal Network (RPN) with a CNN model. It consists of convolution layers, bounding box regression, SoftMax classification, Region of Interest (ROI) pooling, and RPN, enabling accurate detection of oil palm trees [11]. The RPN scans images using anchor boxes and Non-Maximum Suppression [12]. Faster R-CNN outperforms previous models with an accuracy of up to 97.79% in oil palm detection [11]. Additionally, ResNet-50 achieved F1 scores of 95.09% for tree recognition and 92.07% for identifying healthy trees [8]. Faster R-CNN provides high accuracy and efficient processing but requires a large training dataset [13,14].

You Only Look Once (YOLO) is a real-time object detection method with high precision, and it has evolved from YOLOv1 to YOLOv12. [15] highlighted its applications in various fields, while [16] emphasised the need to evaluate which YOLO version performs best. Different YOLO versions have been used in detecting oil palm trees, such as YOLOv5 [17,18] and YOLOv8 [19]. Although promising, a systematic comparison of the latest YOLO models, like YOLOv9, has only been done in other agricultural applications, such as tomatoes.

Based on findings from multiple research studies, YOLO and Faster R-CNN have evolved beyond their previous reliance on object detection across various formats. Faster R-CNN is a two-stage detector, while YOLO is a one-stage detector, indicating that YOLO is faster than Faster R-CNN but less accurate. However, YOLO has advanced recently and now outperforms Faster R-CNN in certain scenarios, such as the detection of oil palm trees. Nevertheless, several academic studies have examined the performance of the YOLO model in its various versions alongside Faster R-CNN, including comparisons between the different YOLO versions and Faster R-CNN. Table 1 summarizes the research gap between the methodologies used for oil palm tree detection and health classification.

Table 1
Research gap between methodologies used for oil palm tree detection and health classification

No	Reference	Data Sources	Methods	Results
1	[8]	A total of 4172 bounding boxes, each containing 2,000 × 2,000-pixel images, depicting unhealthy and healthy palm trees.	• Faster R-CNN • Resnet-50	The identification of oil palm trees, including healthy and unhealthy trees. For visual interpretation ground truth, ResNet-50 achieved F1-scores of 95.09%, 92.07%, and 86.96%; moreover, 97.67%, 95.30%, and 57.14% were also recorded.
2	[11]	The drone services company acquired the UAV data. The images revealed a plantation of oil palm trees covering 22 hectares.	• Faster R-CNN	The total accuracy of oil palm tree detection was evaluated across three different sites, yielding findings of 97.06%, 96.58%, and 97.79% correct oil palm detection, respectively. The results show that the Faster R-CNN method successfully and precisely recognises and counts the number of oil palm plants from the UAV photos.
3	[17]	Data were collected from Papua, Indonesia. The dimensions of the image are 1,024 x 1,024 pixels.	• YOLOv5 • Faster R-CNN • CNNResNet-101	The average F1-score of YOLOv5 is 0.86, outperforming CNNResNet-101 (0.28) and Faster R-CNN (0.56).
4	[18]	Data was collected using UAVs (satellite imagery). The dimensions of this image are 28,062 x 6,377 pixels, with a spatial resolution of 0.27 m.	• YOLOv5 • Faster R-CNN • CNNResNet-101	The average F1-score of YOLOv5 is 0.895, outperforming CNNResNet-101 (0.493) and Faster R-CNN (0.706). With a precision above 96.10% for all classes, YOLOv5 demonstrates its strength, proving it superior to alternative models.
5	[19]	The ripeness of fruit is determined using a diverse dataset that includes 8,299 fresh fruit bunches (FFB) from oil palms.	• YOLOv8 • EfficientDet Lite 4	mAP@50 and mAP@50-95 demonstrated improvements of 4% and 16%, respectively, for YOLO V8s. With mAP values of 0.978 for mAP@50 and 0.765 for mAP@50-95, YOLO V8s surpassed EfficientDet Lite 4.
6	[21]	UAV images	• YOLOv8	A significant advancement in RPW management was realized by integrating the YOLOv8 model for detecting palm trees in UAV images and mapping Red Palm Weevil (RPW), which attained 100% accuracy in RPW detection.

This research benefits the Malaysian government by supporting more effective management of oil palm plantations by detecting unhealthy or stressed oil palm trees early. Such detection can help reduce the spread of pests and diseases, improving crop health and productivity. This aligns with Sustainable Development Goal (SDG) 3, which promotes good health and well-being, as healthier plantations reduce the need for excessive pesticide use and minimize environmental and public health risks. To achieve this, the study is guided by the following objectives:

i. to identify oil palm trees and monitor their health using multispectral images.
ii. to develop a model that is able to detect oil palm trees and classify their health using You Only Look Once (YOLO).
iii. to conduct a comparative evaluation of YOLOv8 and YOLOv9 in detecting and classifying the health of oil palm trees based on performance metrics such as the confusion matrix, precision, recall, F1 score, mean average precision (mAP), loss values, and the precision-recall curve.

This paper is organised as follows: the next section will briefly explain the methods used in this study, including data collection, image preprocessing, and model development, evaluation, and testing for both YOLO models applied. This study's results will be discussed, followed by the conclusion and its limitations.

2. Methodology

A research plan is a comprehensive project overview that includes the researcher's objectives, strategies, schedule, and available resources. A well-crafted research plan is necessary for carrying out a thorough, effective, and morally sound study. It supports researchers in staying on course, making wise choices, and effectively communicating their findings [20]. The research plan comprises six key phases: data collection, image preprocessing, dataset partitioning, model development for health classification, performance evaluation, and model testing. Figure 1 depicts the brief management strategies based on the research plan flowchart.

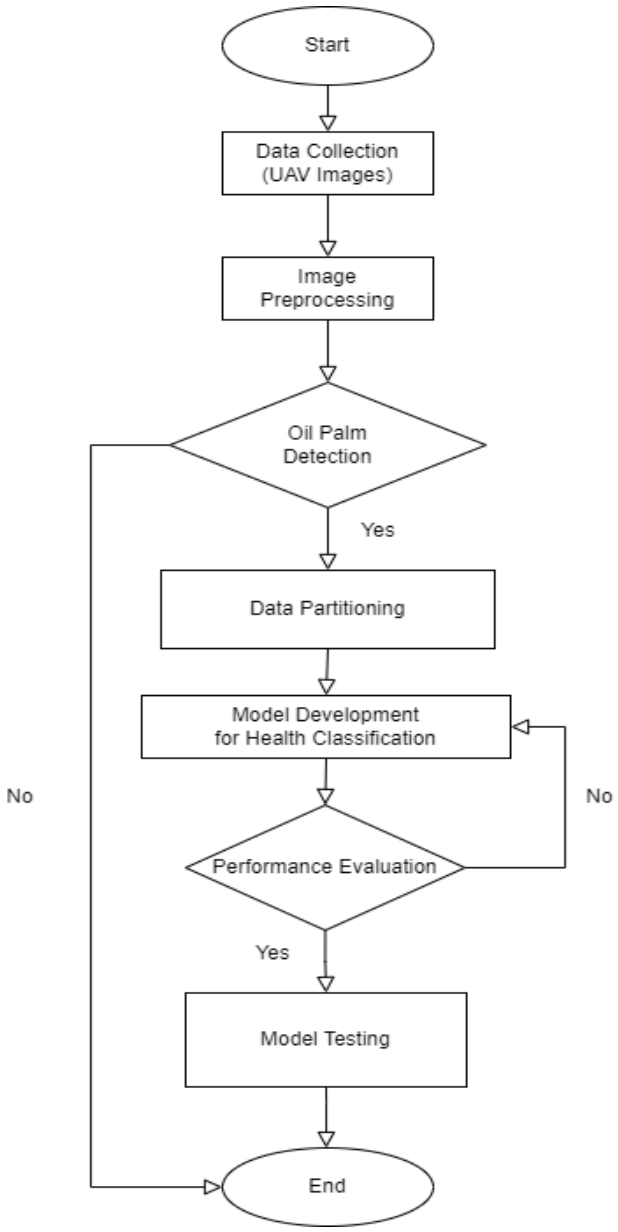

Fig. 1. Research Plan

2.1 Data Collection

The dataset used for this study was provided by MySpatial Sdn Bhd. The study area was in Terengganu, Malaysia. The dataset was represented in UAV multispectral image form by using a drone as a tool for data collection. eBee X is a drone provided by MySpatial, offering 90-minute flights, Real-Time Kinematics (RTK), Post-Processed Kinematics (PPK), online training, and eMotion flight planning software. An external sensor, MicaSense RedEdge-MX, is also attached to the drone. It offers a variety of integration choices, ranging from fully customised integrations to stand-alone options where all that is needed is power for the sensor. For smooth integration with any aircraft, advanced integrations make use of adaptable interfaces, including Ethernet, serial, and PWM/GPIO triggers.

2.2 Image Preprocessing

Image preprocessing transforms raw images into a form that a model is ready to utilise for training and inference, ensuring appropriate structure, cutting down on training time, and speeding up inference. Several preprocessing methods have been applied, which are auto-oriented and resized. Auto-orient removes EXIF data that is attached to the images, discards EXIF rotations, and standardises pixel ordering. Thus, this dataset also applies to resize, which is stretched to 1024 x 1024 pixels.

A bounding box and labelling were used to annotate this dataset. The bounding box is a reference point for object detection, providing the object's position, class, and confidence. Figure 2 shows the labelling in bounding boxes, which have labels on whether it is oil palm trees or not (Palm and Not Palm). After oil palm tree detection, the labelling in the bounding box has two classes, which include healthy and unhealthy for the images that only use oil palm trees.

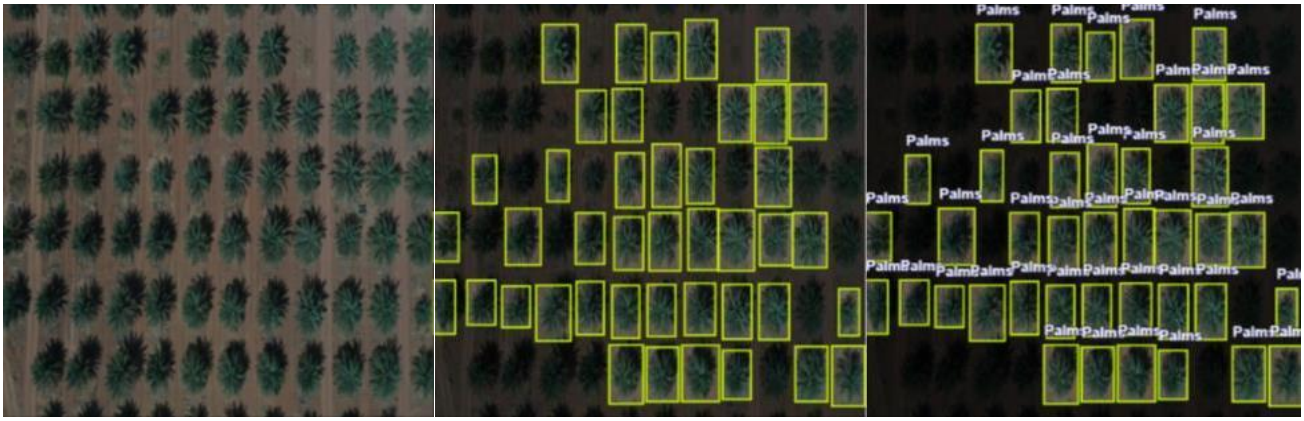

(a) (b) (c)

Fig. 2. (a) UAV image without bounding boxes and labelling; (b) UAV image with bounding boxes; the oil palm tree; and (c) UAV image with bounding boxes and labelling with palms [20]

2.3 Data Partitioning

Data partitioning is splitting the dataset into three parts: train, test, and validation set, to improve the scalability, reduce contention, and optimise performance. In this study, image annotation was applied to the health classification of oil palm trees from UAV multispectral images; the same goes for data augmentation to increase the performance of the models. For this dataset, the data was

partitioned into three parts: 316 images in the training set (70%), 90 images in the validation set (20%), and 44 images in the testing set (10%).

2.4 Model Development for Health Classification

This phase focuses on developing a model to identify palm oil trees and monitor their health using UAV multispectral images. YOLOv9 was chosen for its high accuracy and speed in detecting and classifying healthy and unhealthy palm oil trees, while YOLOv8 was chosen as a comparison to this proposed model. Both models are selected for model development since they are known for their state-of-the-art (SOTA) performance, and all the models will be compared later using the evaluation metrics. By analysing UAV multispectral images, this model can help monitor palm oil plantations and detect potential issues before they become severe.

Based on Table 2, YOLOv8 and YOLOv9 have the same head and backbone of the model architecture, which is YOLO Layer and CSPDarknet53 but are different in the neck. Even though the neck of the model is different, the Path Aggregation Network (PANet) is the feature fusion across various scales and leads to better object detection performance. Programmable Gradient Information (PGI) and Generalized Efficient Layer Aggregation Network (GELAN) are techniques that enhance information flow and feature representation.

Table 2
Model architecture summary of YOLOv8 and YOLOv9

Model	YOLOv8	YOLOv9
Backbone	CSPDarknet53	CSPDarknet53
Neck	PANet	PGI and GELAN
Head	YOLO Layer	YOLO Layer

Eq. (1) shows the loss function that penalises inaccurate predictions and promotes accurate detections by guiding the training process and optimising the detection performance, where each term contributes to distinct parts of the detection job [21].

$$LOSS = L_{classification} + L_{confidence} + L_{CIoU} \quad (1)$$

Table 3 summarises the key differences between the different YOLO models. In conclusion, the object identification method known as You Only Look Once (YOLO) has undergone multiple iterations, each of which has been improved upon from the last.

Table 3
Accuracy and speed in different YOLO models

Model	Speed	Accuracy
YOLOv3	Moderate	High
YOLOv4	Moderate	High
YOLOv5	Fast	Very High
YOLOv6	Moderate	High
YOLOv7	Fast	Very High
YOLOv8	Very Fast	SOTA
YOLOv9	Very Fast	SOTA

2.5 Performance Evaluation

This study employed a confusion matrix, precision, recall, mean average precision (mAP), losses, and a precision-recall curve to evaluate prediction performance, utilising the split test set for a comprehensive evaluation. Figure 3 shows the prediction summary represented in matrix form by the confusion matrix. It assists in identifying the classes that the model is confusing with other classes by displaying the proportion of correct and incorrect predictions for each class [22].

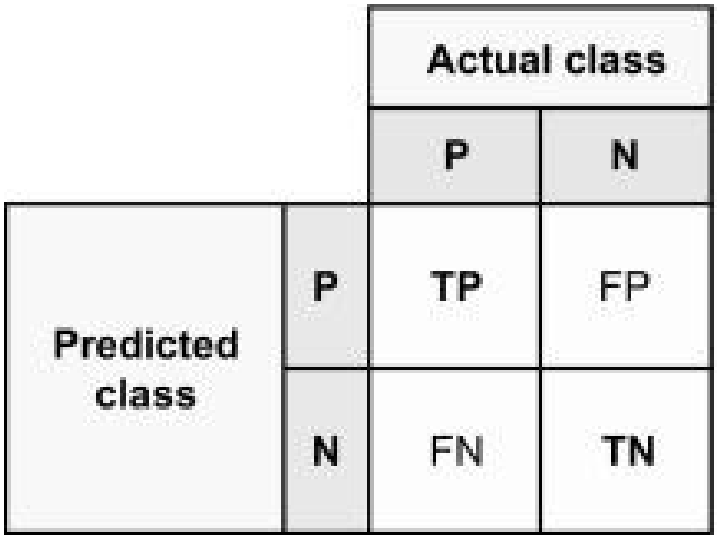

Fig. 3. Confusion matrix [22]

Precision measures the percentage of accurately predicted positive cases, while recall measures how well the model detected the percentage of actual positive cases. Both equations can be found in Eq. (2) and Eq. (3).

$$Precision = \frac{TP}{(TP+FP)} \tag{2}$$

$$Recall = \frac{TP}{(TP+FN)} \tag{3}$$

where TP, FP, and FN represent true positive, false positive, and false negative predictions, respectively.

When evaluating a model's performance for tasks like information retrieval and object detection, mean average precision (mAP) is suggested. mAP formula at Eq. (4).

$$mAP = \frac{1}{N} \sum_{i=1}^{n} AP_i \tag{4}$$

2.6 Model Testing

Model testing is the performance evaluation of the model trained on a new dataset that was not used during training. It helps to identify the problems, such as the model's overfitting, underfitting, and bias, and estimate how well the model can perform on the unseen dataset. It also ensures that this model can perform well and accurately with different datasets.

3. Results

3.1 Data Preparation

UAV multispectral images are huge and challenging to process, including data preprocessing, as shown in Figure 4. Hence, ArcGIS Pro and Global Mapper were used to crop out two areas using clip, buffer, and extract by mask functions in the ArcGIS Pro, as shown in Figure 5 and Figure 6.

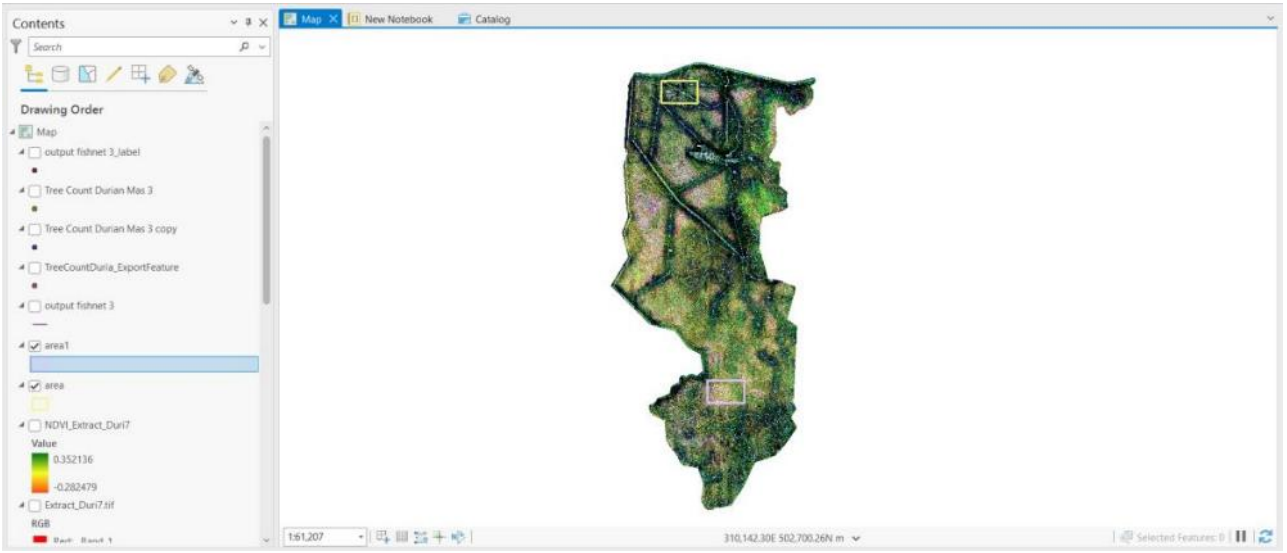

Fig. 4. Full area of UAV multispectral image

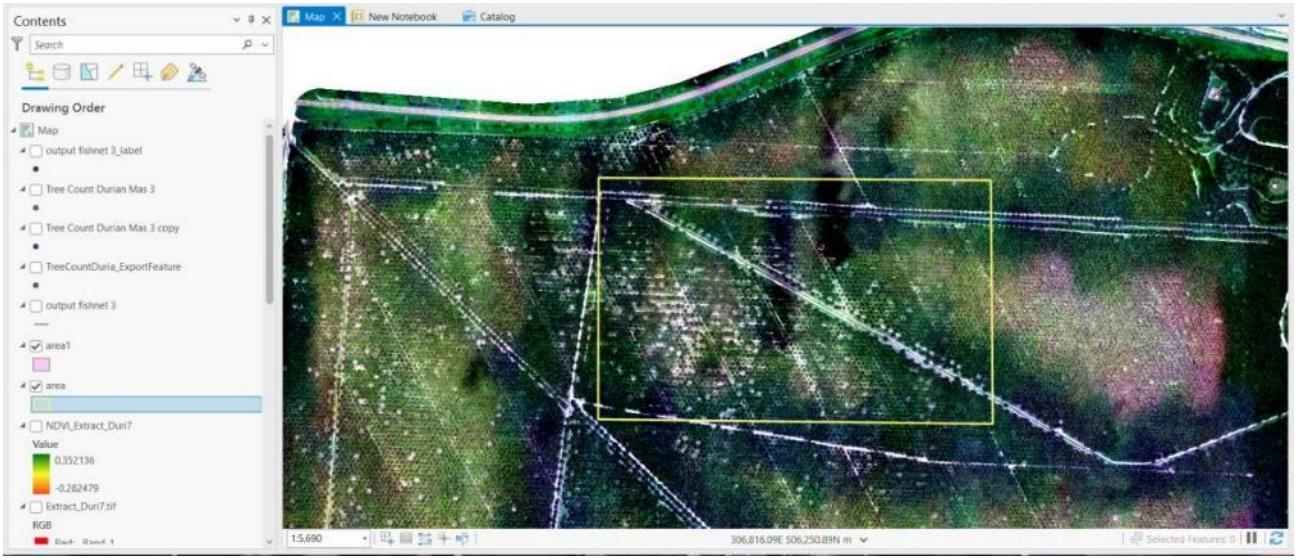

Fig. 5. Area 1 that will be cropped from full UAV multispectral image

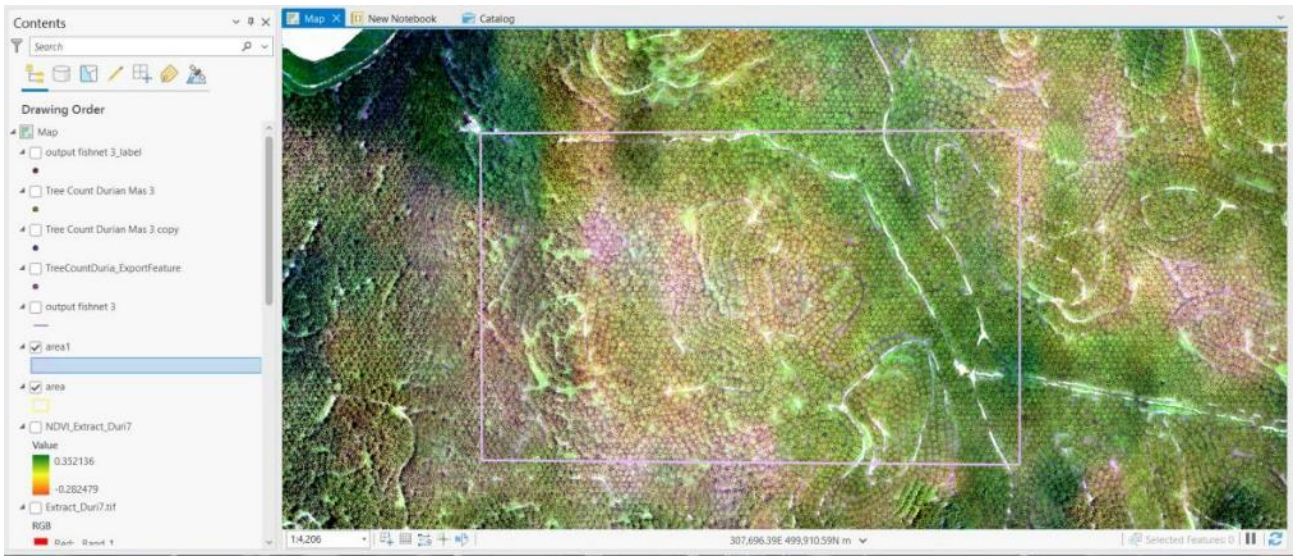

Fig. 6. Area 2 that will be cropped from the full UAV multispectral image

After cropping, the NDVI function was used to calculate the Normalized Difference Red Edge (NDRE) of the plant. It was calculated from near-infrared (NIR) and red-edge wavelengths of light to assess plant health and biomass. Figure 7 and Figure 8 show the NDRE of the plant in the two areas that had been cropped. Additionally, a fishnet tool was used to create a fishnet of rectangular cells; in this case, the output represents polyline features in a 15 x 15 grid for both areas and was visualised in Figure 9 and Figure 10.

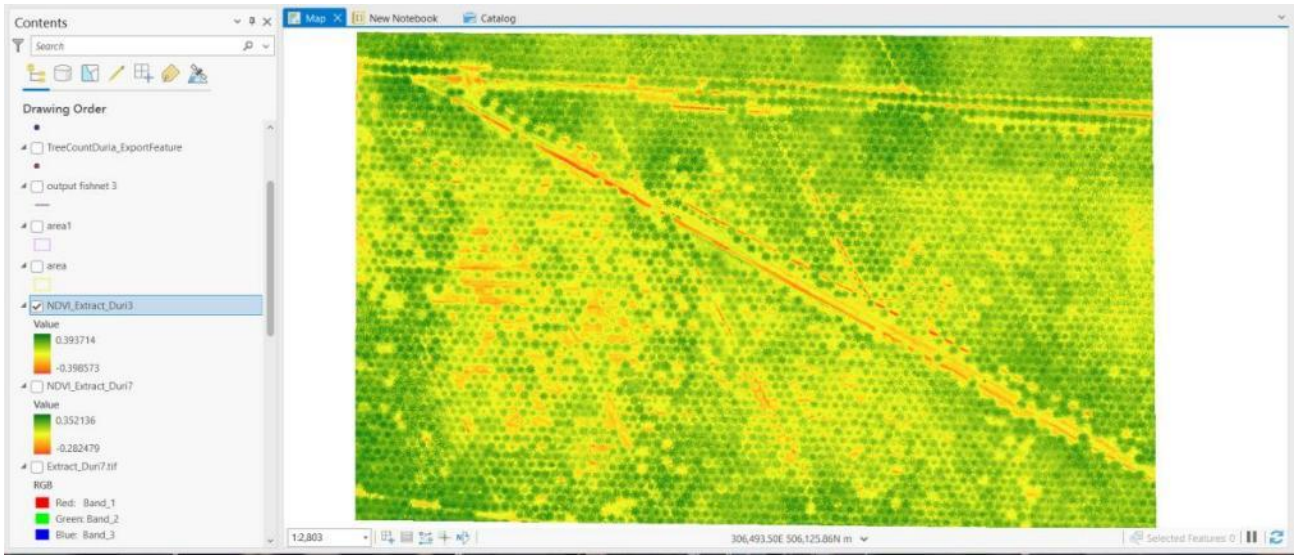

Fig. 7. Area 1 with NDRE of the oil palm tree

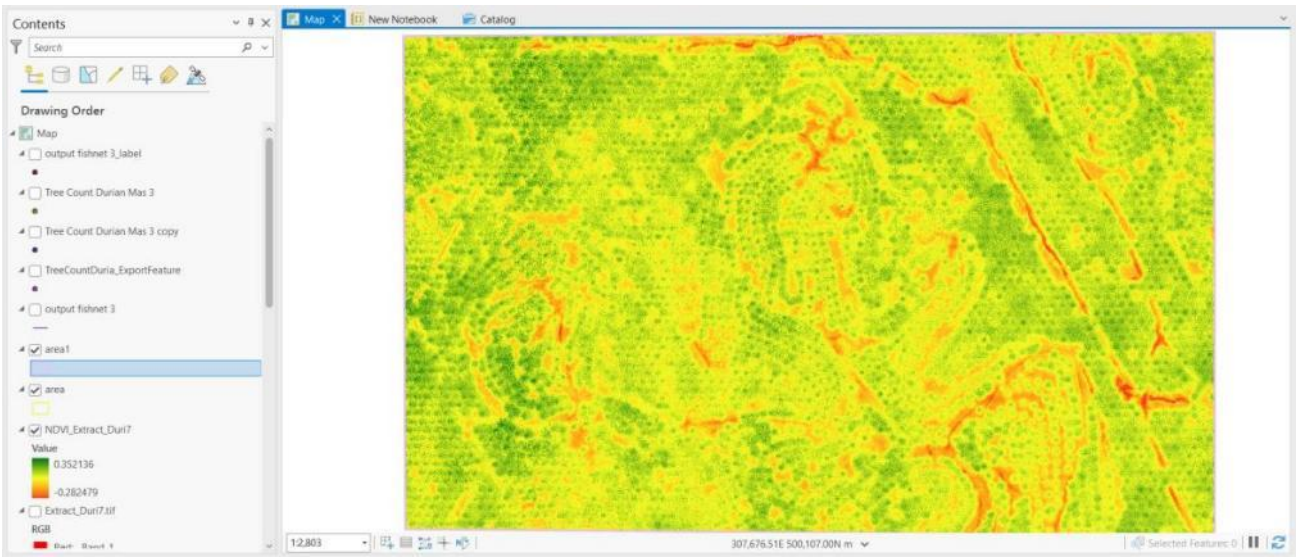

Fig. 8. Area 2 with NDRE of the oil palm tree

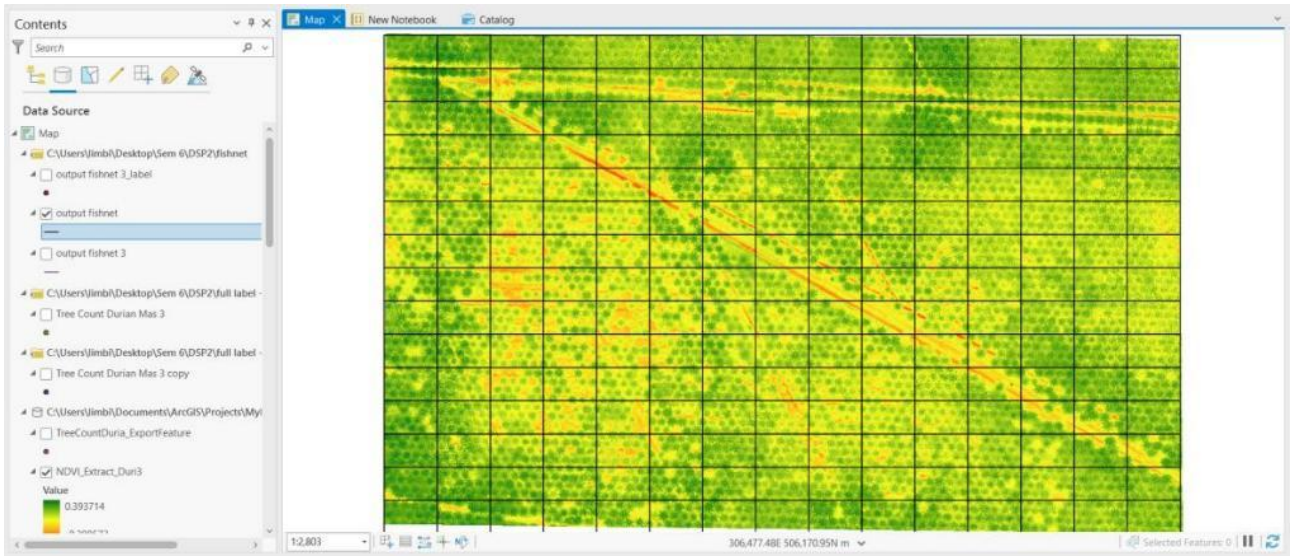

Fig. 9. Area 1 with NDRE and fishnet of the oil palm tree

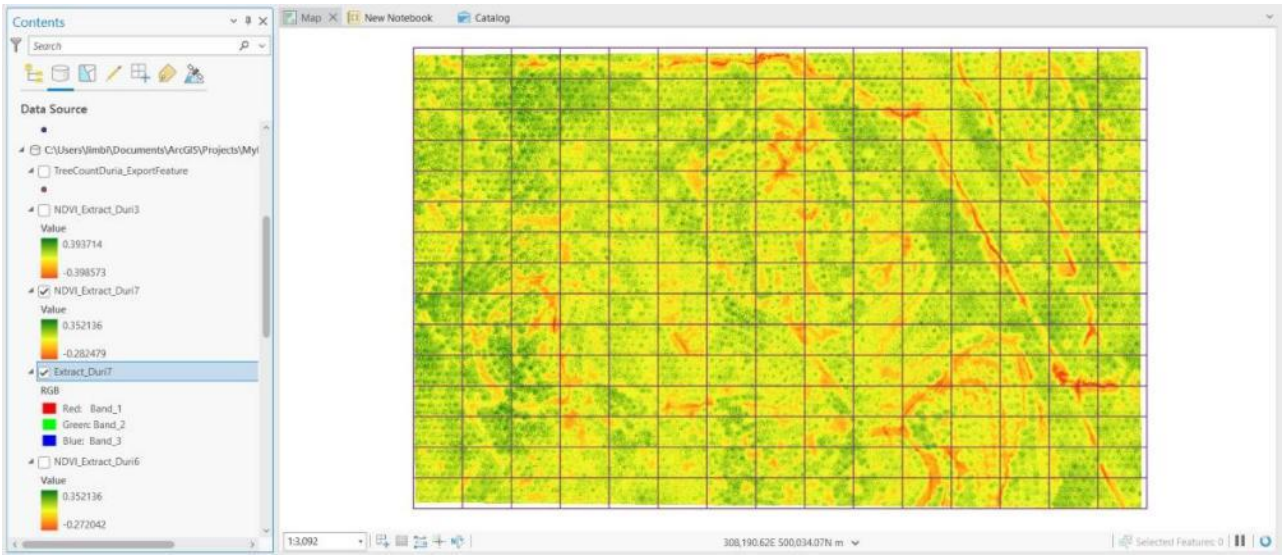

Fig. 10. Area 1 with NDRE and fishnet of the oil palm tree

Both TIF files were imported into Global Mapper to split the area into 15 rows x 15 columns and exported in PNG format. The dataset was imported into Roboflow to proceed with data preprocessing. Figure 11 shows the process of bounding boxes and labelling each oil palm tree in each dataset, where yellow represents healthy trees while blue represents unhealthy trees.

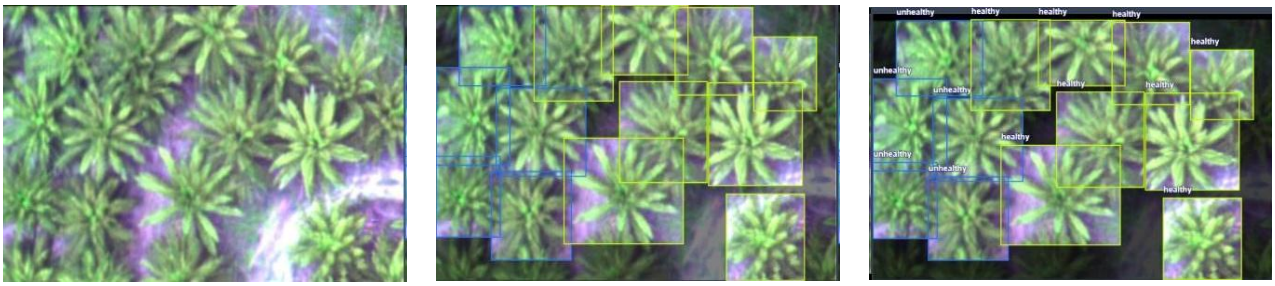

(a) (b) (c)

Fig. 11. (a) UAV multispectral image without bounding boxes and labelling (b) UAV multispectral image with bounding boxes the oil palm tree (c) UAV multispectral image with bounding boxes and labelling with Palms

Subsequently, auto-oriented was applied to discard EXIF rotations, standardise pixel ordering, and resize all the dataset into 640 x 640 pixels. Once data preprocessing was completed, Roboflow automatically generated the dataset and exported it to Google Collab to proceed with model training.

3.2 Model Training

The dataset must be downloaded and saved inside the "{Home}/yolov9" directory and "{Home}/yolov8" directory for YOLOv9 and YOLOv8, respectively, using the dataset API key provided by Roboflow, as shown in Figure 12 for model YOLOv9 and Figure 13 for model YOLOv8.

```
%cd {HOME}/yolov9
/content/yolov9/yolov9

import roboflow

from roboflow import Roboflow
rf = Roboflow(api_key="bLkI2wgqMUzrfPQ8QwZA")
project = rf.workspace("yolov5-mvsln").project("bla-xf2qo")
version = project.version(4)
dataset = version.download("yolov9")
```

Fig. 12. Import dataset from Roboflow for YOLOv9

```
!mkdir {HOME}/datasets
%cd {HOME}/datasets

!pip install roboflow

from roboflow import Roboflow
rf = Roboflow(api_key="bLkI2wgqMUzrfPQ8QwZA")
project = rf.workspace("yolov5-mvsln").project("bla-xf2qo")
version = project.version(4)
dataset = version.download("yolov8")
```

Fig. 13. Import dataset from Roboflow for YOLOv8

Model training for YOLOv9 used a batch size set to 16 and epochs set to 30. However, the dataset is imbalanced, with 1086 instances for healthy and 342 cases for unhealthy, leading to higher recall than precision, as shown in Figure 14 and Figure 15.

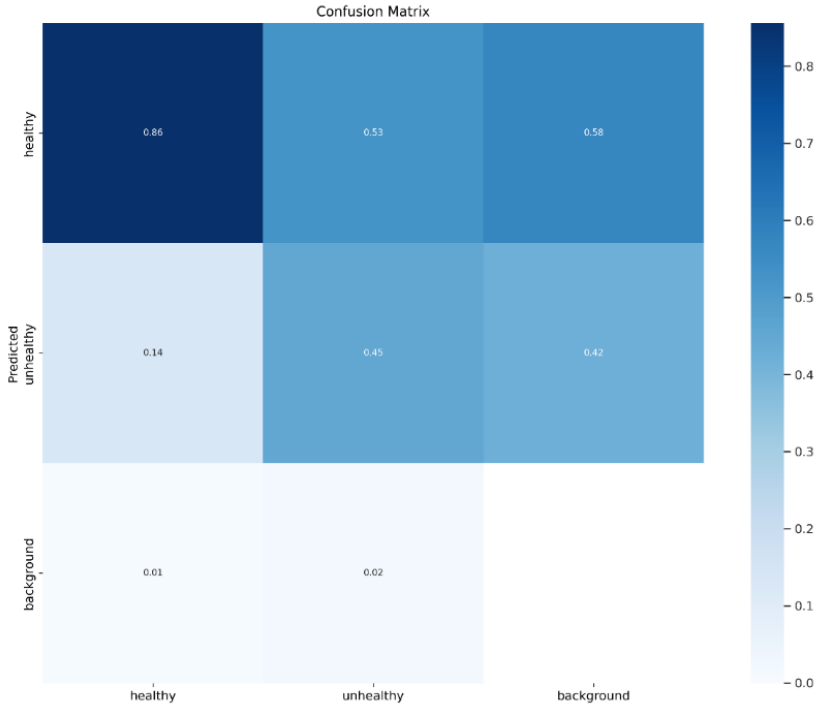

Fig. 14. YOLOv9 confusion matrix

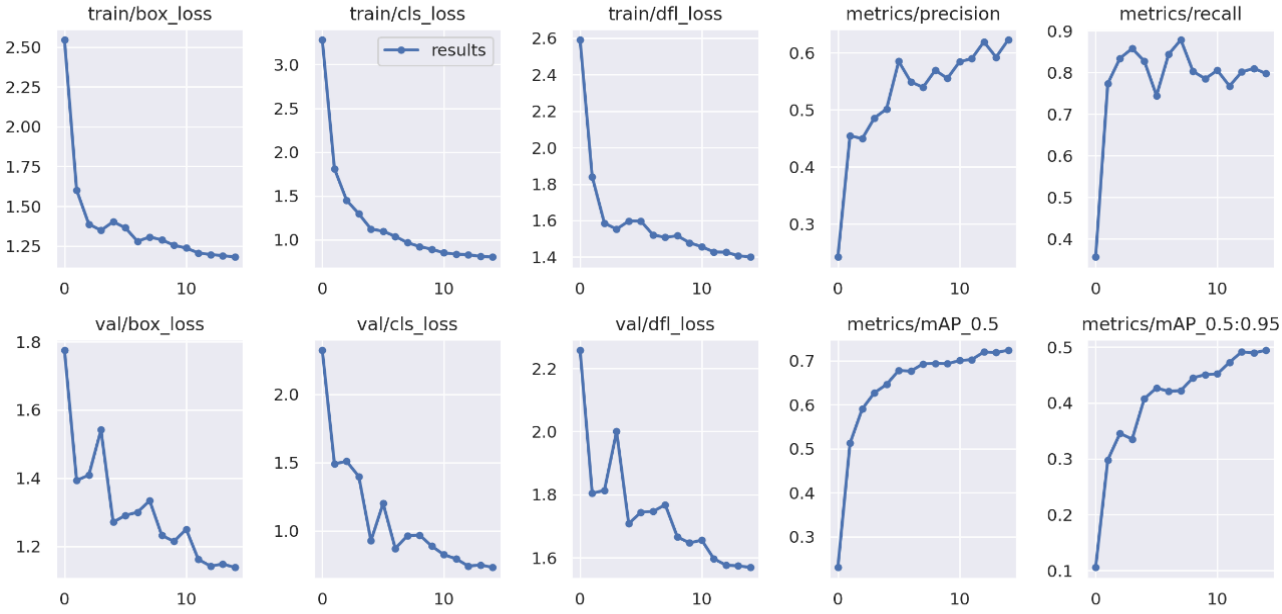

Fig. 15. YOLOv9 overall results

From the experiment conducted using UAV multispectral data, the model is able to predict the healthy oil palm tree, as shown in Figure 16 (a) and Figure 16 (b). Based on the results obtained from this experiment, the model is expected to predict new datasets from another area of UAV multispectral images or other UAV multispectral datasets.

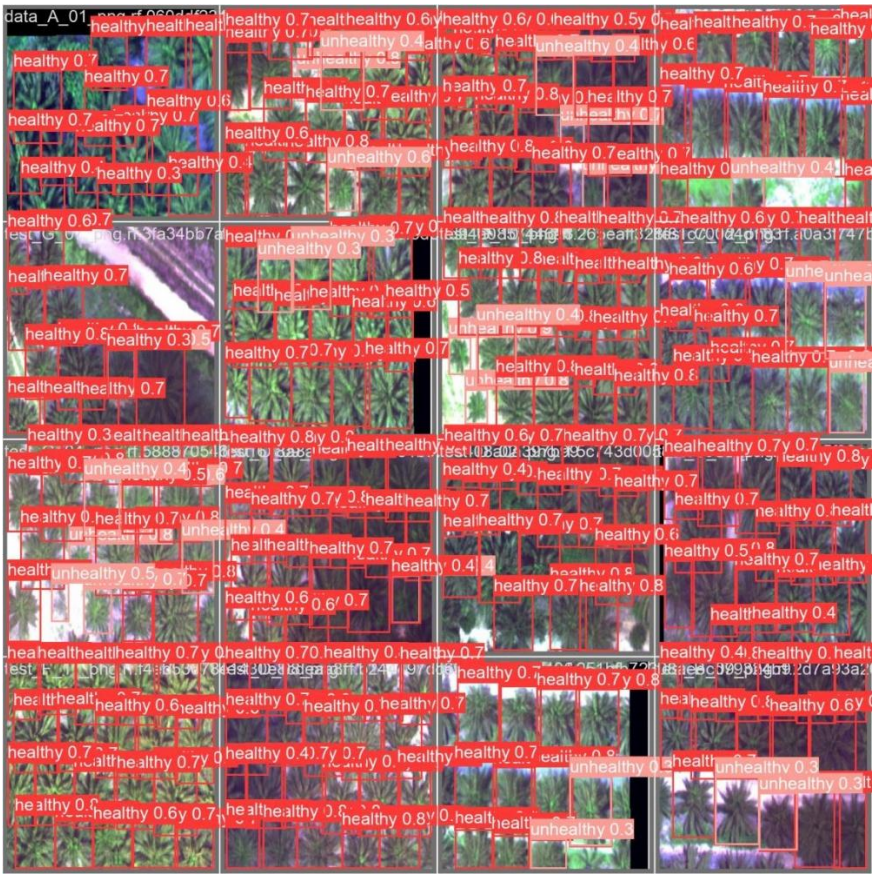

Fig. 16. (a) Oil palm tree health classification by using YOLOv9

Fig. 16. (b) Oil palm tree health classification by using YOLOv9

A similar process was repeated for YOLOv8, where model training for YOLOv8 with specific object detection tasks. The model exhibited the same data imbalance issues, with recall higher than precision, as indicated in Figure 17 and Figure 18.

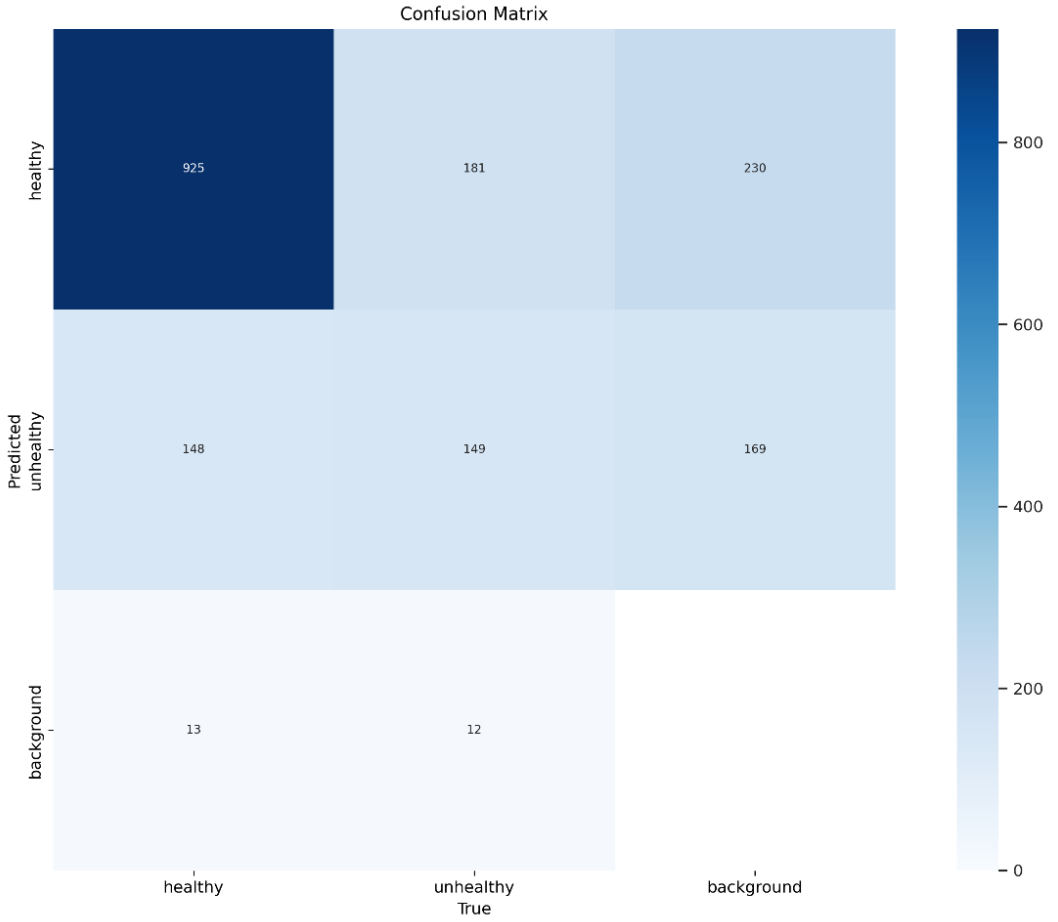

Fig. 17. YOLOv8 confusion matrix

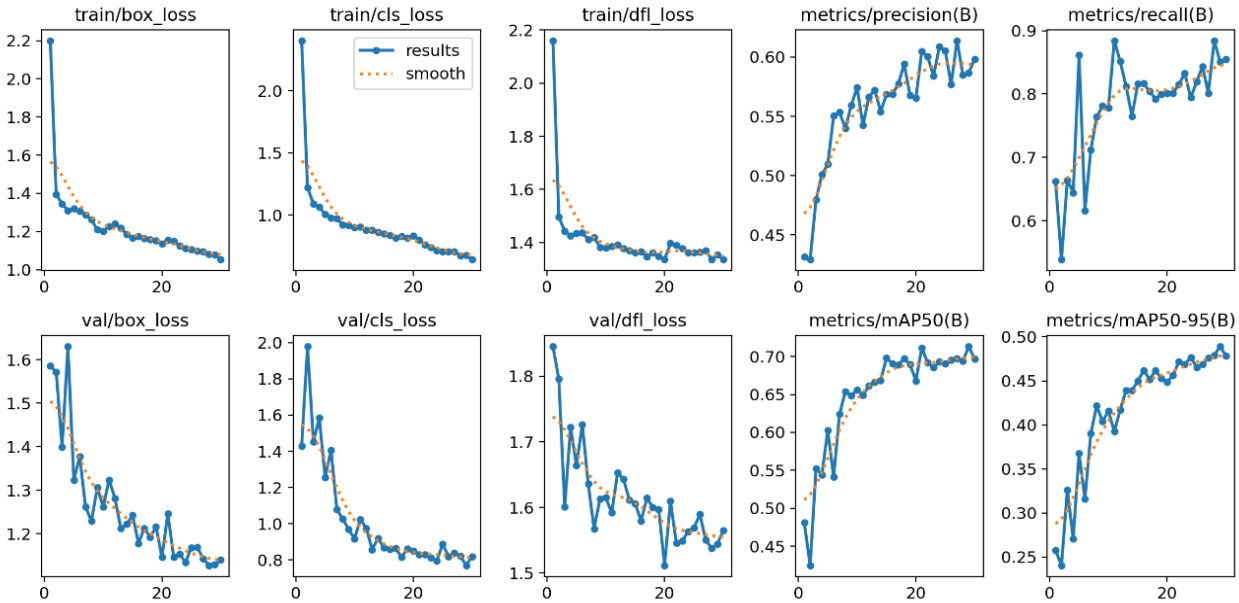

Fig. 18. YOLOv8 overall results

Similar to model YOLOv9, model YOLOv8 is also able to predict the healthy oil palm tree using UAV multispectral images, as shown in Figure 19 (a) and Figure 19 (b).

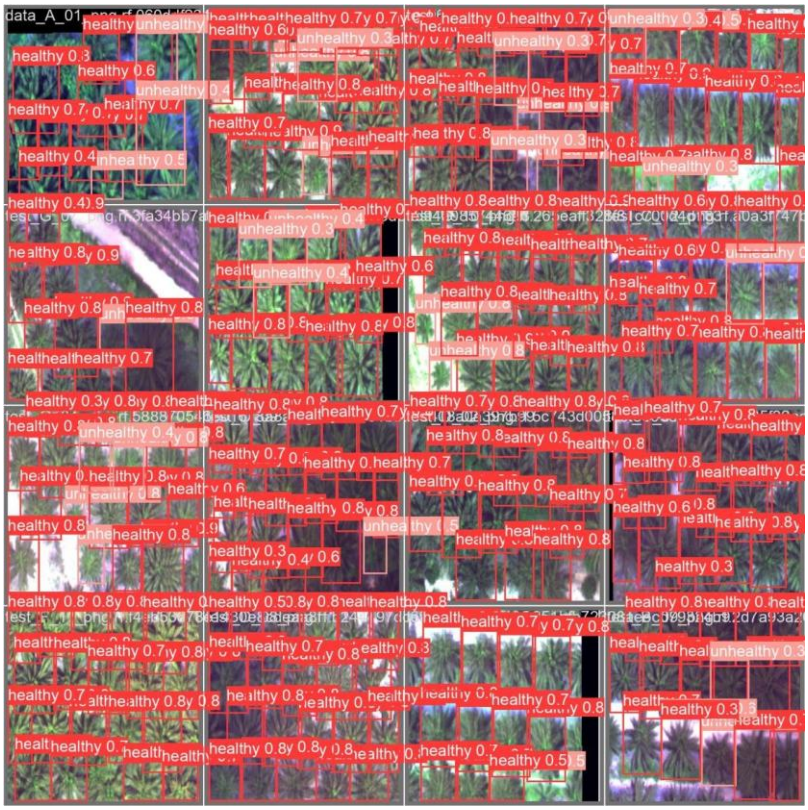

Fig. 19. (a) Oil palm tree health classification by using YOLOv8

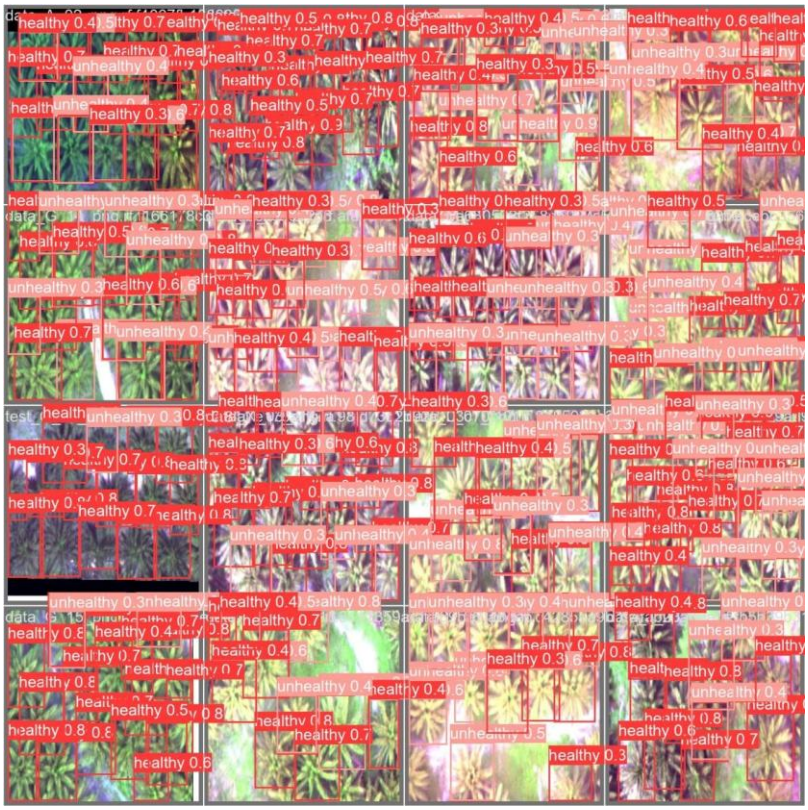

Fig. 19. (b) Oil palm tree health classification by using YOLOv8

3.3 Model Performance Comparison

Table 4 shows the models' performance based on precision, recall, F1 score, mAP50 and mAP50-95. The results from this experiment show that YOLOv9 outperforms YOLOv8 with 0.614 precision, 0.804 recall, 0.696 F1 score, 0.726 mAP50, and 0.502 mAP50-95. Although in terms of computational time, YOLOv8 provides a shorter time compared to YOLOv9, the precision, mAP50, and mAP50-95 for YOLOv8 are all low values compared to YOLOv9. Once the model was developed, the new dataset was used for model testing to determine the model's ability to generalise to new data. Accuracy is frequently utilised in binary or multi-class classification tasks, where each input is classified into a distinct category. Since object detection requires predicting class labels and bounding boxes for several items in a picture, accuracy is a less useful metric.

Table 4
Summary of result

Model	Precision	Recall	F1 score	mAP50	mAP50-95	Time(minutes)
YOLOv8	0.587	0.849	0.694	0.713	0.489	5.1
YOLOv9	0.614	0.804	0.696	0.726	0.502	11.2

3.4 Model Testing

Based on Figure 20 and Figure 21, the output incorporates measures showing how well the model works to identify items of interest, such as precision, recall, and F1-score. The information output can also easily show the number of healthy and unhealthy object detections in each test image. This can be used to assess the model's accuracy in identifying items of interest and differentiating between healthy and unhealthy examples. Additionally, the processing speed of the 55 model was also provided, where the average 109 ms for YOLOv9 and the average 15 ms for YOLOv8 mean that the processing speed for YOLOv8 is faster than YOLOv9. Finally, the model can overlay bounding boxes around detected objects and label them accordingly to assess the accuracy of visual detections.

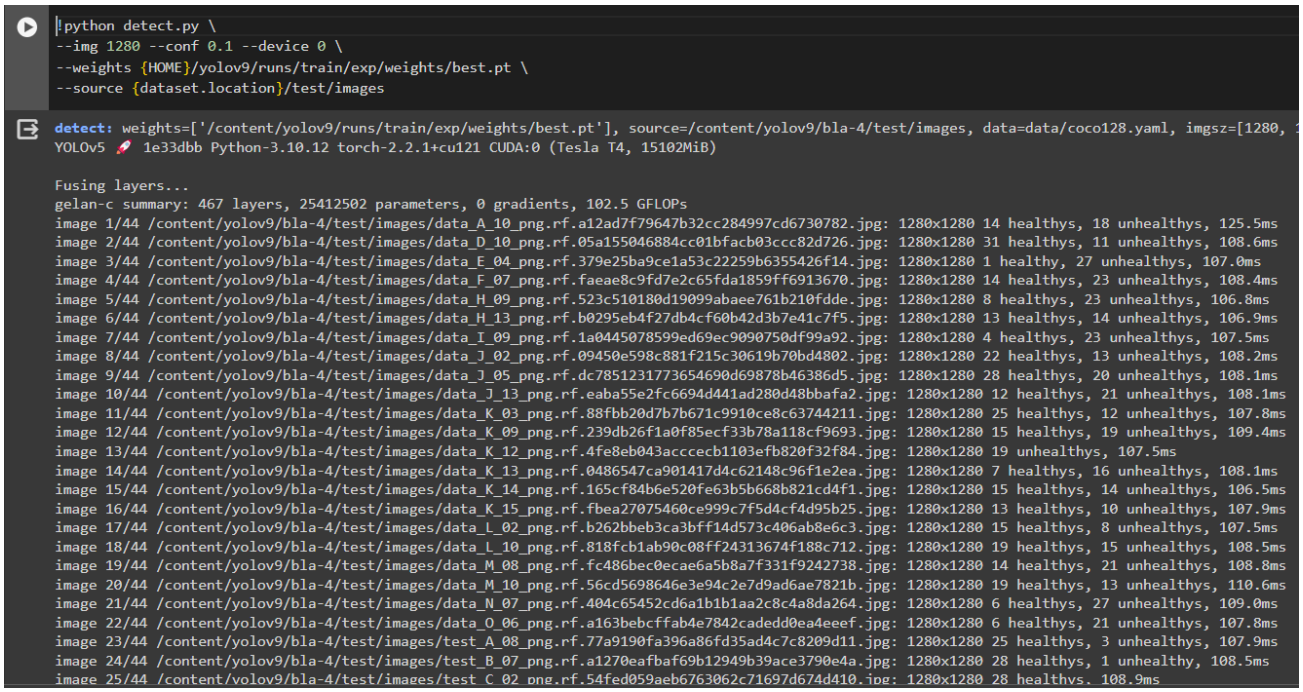

Fig. 20. YOLOv9 model testing

```
%cd {HOME}
!yolo task=detect mode=predict model={HOME}/runs/detect/train/weights/best.pt conf=0.25 source={dataset.location}/test/images save=True

/content
Ultralytics YOLOv8.0.196 🚀 Python-3.10.12 torch-2.2.1+cu121 CUDA:0 (Tesla T4, 15102MiB)
Model summary (fused): 168 layers, 11126358 parameters, 0 gradients, 28.4 GFLOPs

WARNING ⚠️ NMS time limit 0.550s exceeded
image 1/44 /content/datasets/bla-4/test/images/data_A_10_png.rf.a12ad7f79647b32cc284997cd6730782.jpg: 640x640 14 healthys, 11 unhealthys, 16.4ms
image 2/44 /content/datasets/bla-4/test/images/data_D_10_png.rf.05a155046884cc01bfacb03ccc82d726.jpg: 640x640 22 healthys, 2 unhealthys, 16.4ms
image 3/44 /content/datasets/bla-4/test/images/data_E_04_png.rf.379e25ba9ce1a53c22259b6355426f14.jpg: 640x640 7 healthys, 20 unhealthys, 16.3ms
image 4/44 /content/datasets/bla-4/test/images/data_F_07_png.rf.faeae8c9fd7e2c65fda1859ff6913670.jpg: 640x640 12 healthys, 13 unhealthys, 16.3ms
image 5/44 /content/datasets/bla-4/test/images/data_H_09_png.rf.523c510180d19099abaee761b210fdde.jpg: 640x640 14 healthys, 10 unhealthys, 16.3ms
image 6/44 /content/datasets/bla-4/test/images/data_H_13_png.rf.b0295eb4f27db4cf60b42d3b7e41c7f5.jpg: 640x640 15 healthys, 6 unhealthys, 16.3ms
image 7/44 /content/datasets/bla-4/test/images/data_I_09_png.rf.1a0445078599ed69ec9090750df99a92.jpg: 640x640 10 healthys, 11 unhealthys, 16.3ms
image 8/44 /content/datasets/bla-4/test/images/data_J_02_png.rf.09450e598c881f215c30619b70bd4802.jpg: 640x640 20 healthys, 1 unhealthy, 16.3ms
image 9/44 /content/datasets/bla-4/test/images/data_J_05_png.rf.dc7851231773654690d69878b46386d5.jpg: 640x640 24 healthys, 3 unhealthys, 16.3ms
image 10/44 /content/datasets/bla-4/test/images/data_J_13_png.rf.eaba55e2fc6694d441ad280d48bbafa2.jpg: 640x640 10 healthys, 8 unhealthys, 16.1ms
image 11/44 /content/datasets/bla-4/test/images/data_K_03_png.rf.88fbb20d7b7b671c9910ce8c63744211.jpg: 640x640 18 healthys, 15.3ms
image 12/44 /content/datasets/bla-4/test/images/data_K_09_png.rf.239db26f1a0f85ecf33b78a118cf9693.jpg: 640x640 8 healthys, 11 unhealthys, 15.3ms
image 13/44 /content/datasets/bla-4/test/images/data_K_12_png.rf.4fe8eb043acccecb1103efb820f32f84.jpg: 640x640 2 healthys, 15 unhealthys, 15.3ms
image 14/44 /content/datasets/bla-4/test/images/data_K_13_png.rf.0486547ca901417d4c62148c96f1e2ea.jpg: 640x640 6 healthys, 12 unhealthys, 15.3ms
image 15/44 /content/datasets/bla-4/test/images/data_K_14_png.rf.165cf84b6e520fe63b5b668b821cd4f1.jpg: 640x640 13 healthys, 5 unhealthys, 15.3ms
image 16/44 /content/datasets/bla-4/test/images/data_K_15_png.rf.fbea27075460ce999c7f5d4cf4d95b25.jpg: 640x640 15 healthys, 3 unhealthys, 14.7ms
image 17/44 /content/datasets/bla-4/test/images/data_L_02_png.rf.b262bbeb3ca3bff14d573c406ab8e6c3.jpg: 640x640 13 healthys, 3 unhealthys, 14.7ms
image 18/44 /content/datasets/bla-4/test/images/data_L_10_png.rf.818fcb1ab90c08ff24313674f188c712.jpg: 640x640 16 healthys, 15 unhealthys, 14.7ms
image 19/44 /content/datasets/bla-4/test/images/data_M_08_png.rf.fc486bec0ecae6a5b8a7f331f9242738.jpg: 640x640 19 healthys, 3 unhealthys, 14.7ms
image 20/44 /content/datasets/bla-4/test/images/data_M_10_png.rf.56cd5698646e3e94c2e7d9ad6ae7821b.jpg: 640x640 17 healthys, 5 unhealthys, 14.7ms
image 21/44 /content/datasets/bla-4/test/images/data_N_07_png.rf.404c65452cd6a1b1b1aa2c8c4a8da264.jpg: 640x640 16 healthys, 10 unhealthys, 14.7ms
image 22/44 /content/datasets/bla-4/test/images/data_O_06_png.rf.a163bebcffab4e7842cadedd0ea4eeef.jpg: 640x640 13 healthys, 7 unhealthys, 14.8ms
image 23/44 /content/datasets/bla-4/test/images/test_A_08_png.rf.77a9190fa396a86fd35ad4c7c8209d11.jpg: 640x640 18 healthys, 14.8ms
```

Fig. 21. YOLOv8 model testing

This section provided a detailed analysis, results, and discussion of the objectives analysis, which are to develop a deep learning model that can identify palm oil and monitor the health of oil palm trees from UAV multispectral images, evaluate the proposed model's performance based on metrics such as confusion matrix, precision, recall, mean average precision (mAP), losses, and precision-recall curve and compare the performance with other YOLO version. Based on the results, YOLOv9 outperforms YOLOv8.

4. Conclusion

This study addresses the challenges faced by the palm oil industry, including pest-related diseases, damage caused by rats, and the impacts of climate change. Recognising Malaysia's significant role as the second-largest palm oil exporter globally, the government allocated RM100 million in the 2024 Budget to enhance palm oil production. To tackle these challenges, the study proposed an approach utilising remote sensing technology, specifically the You Only Look Once (YOLO) model, to monitor the health of oil palm trees.

The primary objectives of the study were threefold. Firstly, the aim was to identify and monitor the health of palm oil trees using UAV multispectral images. Secondly, the research sought to develop a YOLO-based model, specifically YOLOv9, to identify and monitor the health of oil palm trees from UAV multispectral images. Finally, the study aimed to evaluate the proposed model's performance, employing metrics such as the confusion matrix, precision, recall, and mean average precision (mAP). Additionally, the performance of YOLOv9 was compared with other YOLO versions, namely YOLOv8.

Furthermore, this study has achieved all the objectives and provided valuable insights into assessing, analysing, and monitoring palm oil trees' health. The discoveries present a substantial opportunity to increase the palm oil industry's productivity and sustainability using cutting-edge technology.

However, several limitations were identified in this study. Bounding box annotation and labelling is a particularly important but difficult phase often carried out by hand to assure accuracy. Automated systems for these tasks can sometimes produce unsatisfactory results because they have

difficulty correctly interpreting diverse or complex images, leading to errors during model training. Manual annotation ensures the quality and dependability of the dataset by precisely identifying and naming the objects inside the photos, but it is time-consuming. Furthermore, the dataset collected is imbalanced, meaning the labelling of healthy and unhealthy oil palm trees is very different. Also, it is important to acknowledge the potential challenges associated with using real datasets in future projects, such as variations in image quality, drone flight altitude, and weather conditions. These factors can significantly impact model accuracy, emphasising the need for robust preprocessing techniques to ensure reliable results.

Several recommendations are proposed for future research to address the limitations identified in this study. First, adopting semi-automated or AI-assisted annotation tools is encouraged to reduce the time and effort involved in manual bounding box labelling while maintaining accuracy. Additionally, expanding and balancing the dataset by collecting a more significant number of images that represent both healthy and unhealthy oil palm trees is crucial. Techniques such as data augmentation and synthetic image generation can further help address class imbalance. To minimize inconsistencies arising from image quality, drone altitude, and weather conditions, it is recommended to standardize data collection protocols and UAV flight settings. Incorporating robust image preprocessing techniques such as normalization, contrast enhancement, and noise reduction can also improve model reliability and accuracy under varying environmental conditions. Furthermore, exploring multimodal approaches by integrating multispectral images with data from other sources, such as thermal imagery or environmental sensors, may provide a more comprehensive assessment of oil palm tree health. Lastly, future research should consider developing a continuous model training and deployment pipeline within a real-time monitoring system to support proactive and efficient plantation management.

Acknowledgment

This research was not funded by any grant. However, the dataset for this study was provided by MySpatial Sdn. Bhd.

References

[1] Mohd Hanafiah, Khayriyyah, Aini Hasanah Abd Mutalib, Priscillia Miard, Chun Sheng Goh, Shahrul Anuar Mohd Sah, and Nadine Ruppert. “Impact of Malaysian Palm Oil on Sustainable Development Goals: Co-Benefits and Trade-Offs across Mitigation Strategies.” *Sustainability Science* 17, no. 4 (October 15, 2021). https://doi.org/10.1007/s11625-021-01052-4

[2] Murphy, Denis J., Kirstie Goggin, and R. Russell M. Paterson. “Oil Palm in the 2020s and Beyond: Challenges and Solutions.” *CABI Agriculture and Bioscience* 2, no. 1 (October 11, 2021). https://doi.org/10.1186/s43170-021-00058-3

[3] Wong, W.C., Tung, H.J., Nurul Fadhilah, M., Midot, F., Lau, L., Melling, L., Astari, S. “Evidence for High Gene Flow, Nonrandom Mating, and Genetic Bottlenecks of Ganoderma Boninense Infecting Oil Palm (Elaeis Guineensis Jacq.) Plantations in Malaysia and Indonesia.” *Mycologia* 114, no. 6 (October 14, 2022): 947–63. https://doi.org/10.1080/00275514.2022.2118512

[4] Paterson, R. Russell M., and Nelson Lima. “Climate Change Affecting Oil Palm Agronomy, and Oil Palm Cultivation Increasing Climate Change, Require Amelioration.” *Ecology and Evolution* 8, no. 1 (November 30, 2017): 452–61. https://doi.org/10.1002/ece3.3610

[5] Phua, M.-H., Chong, C.W., Ahmad, A.H. and Hafidzi, M.N. “Understanding Rat Occurrences in Oil Palm Plantation Using High-Resolution Satellite Image and GIS Data.” *Precision Agriculture* 19, no. 1 (January 10, 2017): 42–54. https://doi.org/10.1007/s11119-016-9496-z

[6] Mohd Noh, Ariff Ateed. “FIELD EFFICACY of ANTICOAGULANT RODENTICIDES against RAT INFESTATION in OIL PALM PLANTATION.” *Journal of Oil Palm Research* (August 11, 2022). https://doi.org/10.21894/jopr.2022.0044

[7] Chung, Gait Fee. “Effect of Pests and Diseases on Oil Palm Yield.” *Palm Oil* (2012): 163–210. https://doi.org/10.1016/b978-0-9818936-9-3.50009-5

[8] Yarak, Kanitta, Apichon Witayangkurn, Kunnaree Kritiyutanont, Chomchanok Arunplod, and Ryosuke Shibasaki. "Oil Palm Tree Detection and Health Classification on High-Resolution Imagery Using Deep Learning." *Agriculture* 11, no. 2 (February 23, 2021): 183. https://doi.org/10.3390/agriculture11020183

[9] Akinkuolie, Timothy, A., Timothy, O., Ogunbode, and Victor O Oyebamiji. "Evaluating Constraints Associated with Farmers' Adaptation Strategies to Climate Change Impact on Farming in The Tropical Environment." *Heliyon* 10, no. 16 (August 1, 2024): e36086–86. https://doi.org/10.1016/j.heliyon.2024.e36086

[10] Hossamelden Mohamed Elhawary, Mohd Ibrahim Shapiai, Upendra Suddamalla, Anthony Wong, & Hairi Zamzuri. "Shape-based Single Stage Deep Neural Network for Traffic Sign Applications." *Journal of Advanced Research in Computing and Applications* 28, no. 1 (2024): 12–24.

[11] Liu, Xinni, Kamarul Hawari Ghazali, Fengrong Han, and Izzeldin Ibrahim Mohamed. "Automatic Detection of Oil Palm Tree from UAV Images Based on the Deep Learning Method." *Applied Artificial Intelligence* 35, no. 1 (October 22, 2020): 13–24. https://doi.org/10.1080/08839514.2020.1831226

[12] Zheng, Juepeng, Haohuan Fu, Weijia Li, Wenzhao Wu, Le Yu, Shuai Yuan, Wai Yuk William Tao, Tan Kian Pang, and Kasturi Devi Kanniah. "Growing Status Observation for Oil Palm Trees Using Unmanned Aerial Vehicle (UAV) Images." *ISPRS Journal of Photogrammetry and Remote Sensing* 173 (March 2021): 95–121. https://doi.org/10.1016/j.isprsjprs.2021.01.008

[13] Zheng, Juepeng, Weijia Li, Maocai Xia, Runmin Dong, Haohuan Fu, and Shuai Yuan. "Large-Scale Oil Palm Tree Detection from High-Resolution Remote Sensing Images Using Faster-RCNN," July 1, 2019. https://doi.org/10.1109/igarss.2019.8898360

[14] Xiang, Ang Jin, Aqilah Baseri Huddin, Mohd Faisal Ibrahim, and Fazida Hanim Hashim. "An Oil Palm Loose Fruits Image Detection System Using Faster R -CNN and Jetson TX2." *IEEE Xplore*, October 1, 2021. https://doi.org/10.1109/ICEEI52609.2021.9611111

[15] Górriz, Juan M., Javier Ramírez, Andrés Ortíz, Francisco J. Martínez-Murcia, Fermin Segovia, John Suckling, Matthew Leming, et al. "Artificial Intelligence within the Interplay between Natural and Artificial Computation: Advances in Data Science, Trends and Applications." *Neurocomputing* 410, no. 2 (October 2020): 237–70. https://doi.org/10.1016/j.neucom.2020.05.078

[16] Olorunshola, Oluwaseyi Ezekiel, Martins Ekata Irhebhude, and Abraham Eseoghene Evwiekpaefe. "A Comparative Study of YOLOv5 and YOLOv7 Object Detection Algorithms." *Journal of Computing and Social Informatics* 2, no. 1 (February 8, 2023): 1–12. https://doi.org/10.33736/jcsi.5070.2023

[17] Desta Sandya Prasvita, Aniati Murni Arymurthy, and Dina Chahyati. "Deep Learning Model for Automatic Detection of Oil Palm Trees in Indonesia with YOLO-V5," October 24, 2023. https://doi.org/10.1145/3626641.3626924

[18] Nuwara, Yohanes, W. K. Wong, and Filbert H. Juwono. "Modern Computer Vision for Oil Palm Tree Health Surveillance Using YOLOv5." *IEEE Xplore*, October 1, 2022. https://doi.org/10.1109/GECOST55694.2022.10010668

[19] Muhammad, and Suharjito Suharjito. "Comparison of YOLOv8 and EfficientDet4 Algorithms in Detecting the Ripeness of Oil Palm Fruit Bunch," September 6, 2023. https://doi.org/10.1109/iciss59129.2023.10291928

[20] Ennis, Catherine D. "A Theoretical Framework: The Central Piece of a Research Plan." *Journal of Teaching in Physical Education* 18, no. 2 (January 1999): 129–40. https://doi.org/10.1123/jtpe.18.2.129

[21] Hajjaji, Yosra, Ayyub Alzahem, Wadii Boulila, Imed Riadh Farah, and Anis Koubaa. "Sustainable Palm Tree Farming: Leveraging IoT and Multi-Modal Data for Early Detection and Mapping of Red Palm Weevil." *ArXiv (Cornell University)*, January 1, 2023. https://doi.org/10.48550/arxiv.2306.16862

[22] Tiwari, Ashish. "Supervised Learning: From Theory to Applications." *Elsevier EBooks*, January 1, 2022, 23–32. https://doi.org/10.1016/b978-0-12-824054-0.00026-5